European Journal of Pharmacology 886 (2020) 173413

Contents lists available at ScienceDirect

European Journal of Pharmacology

journal homepage: www.elsevier.com/locate/ejphar

Full length article

Distinct effects on cAMP signaling of carbamazepine and its structural derivatives do not correlate with their clinical efficacy in epilepsy

Sara Krarup [a,1], Christoffer Mertz [a,1], Emil Jakobsen [a], Sandy E.H. Lindholm [a], Lars H. Pinborg [b], Lasse K. Bak [a,*]

[a] Department of Drug Design and Pharmacology, Faculty of Health and Medical Sciences, University of Copenhagen, 2100, Copenhagen, Denmark
[b] Epilepsy Clinic and Neurobiology Research Unit, Copenhagen University Hospital, University of Copenhagen, 2100, Copenhagen, Denmark

ARTICLE INFO

Keywords:
Epilepsy
cAMP
AC8
Carbamazepine
Oxcarbazepine
Eslicarbazepine

ABSTRACT

The antiepileptic sodium channel blocker, carbamazepine, has long been known to be able to attenuate cAMP signals. This could be of clinical importance since cAMP signaling has been shown to be involved in epileptogenesis and seizures. However, no information on the ability to affect cAMP signaling is available for the marketed structural derivatives, oxcarbazepine and eslicarbazepine acetate or their dominating metabolite, licarbazepine. Thus, we employed a HEK293 cell line stably expressing a cAMP biosensor to assess the effect of these two drugs on cAMP accumulation. We find that oxcarbazepine does not affect cAMP accumulation whereas eslicarbazepine acetate, surprisingly, is able to enhance cAMP accumulation. Since the transcription of *ADCY8* (adenylyl cyclase isoform 8; AC8) has been found to be elevated in epileptic tissue from patients, we subsequently expressed AC8 in the HEK293 cells. In the AC8-expressing cells, oxcarbazepine was now able to attenuate whereas eslicarbazepine maintained its ability to increase cAMP accumulation. However, at all concentrations tested, licarbazepine demonstrated no effect on cAMP accumulation. Thus, we conclude that the effects exerted by carbamazepine and its derivatives on cAMP accumulation do not correlate with their clinical efficacy in epilepsy. However, this does not disqualify cAMP signaling *per se* as a potential disease-modifying drug target for epilepsy since more potent and selective inhibitors may be of therapeutic value.

1. Introduction

The classic antiepileptic drug (AED) carbamazepine (CBZ) has multiple mechanisms-of-action but the one thought to be relevant for its therapeutic effect in epilepsy is stabilization/inhibition of voltage-gated sodium channels (Ambrósio et al., 2002). In addition to epilepsy, CBZ has also proven valuable in the treatment of neuropathic pain and affective disorders (Spina and Perugi, 2004). Interestingly, we have known for decades that CBZ (and other AEDs) is able to affect cAMP signaling in cells and brain tissue (e.g. Chen et al., 1996; Ferrendelli and Kinscherf, 1979; Mann et al., 2009; Palmer et al., 1979) and that cAMP signaling likely plays a somewhat complex role in both epileptogenesis and propagation of seizures (review, Mertz et al., 2020). However, the potential therapeutic role of this mechanism-of-action of CBZ has not been fully established nor has any AEDs specifically targeting the cAMP signaling system been developed. Substantiating the potential role of cAMP in epilepsy, we recently found a number of genes related to the cAMP signaling system to be differentially transcribed in the hippocampus of patients suffering from drug-resistant mesial temporal lobe epilepsy (Guelfi et al., 2019; Kjaer et al., 2019). The etiology related to this observation remains to be established; however, this and other evidence (as reviewed recently by Mertz et al., 2020) strongly suggests a role of cAMP signaling in epilepsy yet to be exploited for drug discovery.

One key step towards evaluating cAMP signaling as a novel drug target is to perform back-translational studies to map the existing AEDs' effect on the cAMP signaling system and the potential contribution of this to the therapeutic effects. To begin to address this, we here test the ability of CBZ and its structural derivatives oxcarbazepine (OXC) or eslicarbazepine acetate (ESL), as well as the dominating active metabolite of OXC and ESL, (R)- and (S)-licarbazepine (LIC), to attenuate cAMP accumulation in a cell-based model system (chemical structures are shown in Fig. 1). OXC and ESL were developed with the purpose of obtaining a more preferable adverse effect profile as compared to CBZ while retaining the desired therapeutic effects (Ambrósio et al., 2002).

* Corresponding author.
E-mail address: laba@sund.ku.dk (L.K. Bak).
[1] Shared first authorship.

https://doi.org/10.1016/j.ejphar.2020.173413
Received 6 March 2020; Received in revised form 7 July 2020; Accepted 23 July 2020
Available online 3 August 2020

Further, we specifically evaluate the ability of CBZ, OXC, ESL or LIC to affect cAMP accumulation driven by the enzyme adenylyl cyclase isoform 8 (AC8). We previously found that this AC isoform was the only one of the nine isoforms of plasmamembrane-bound ACs whose transcription was up-regulated in the hippocampus of patients with drug-resistant mesial temporal lobe epilepsy (Kjaer et al., 2019) suggesting that AC8 could be at least partly responsible for increased cAMP signaling in epileptogenesis and/or for driving seizures. Finally, we discuss the complex pharmacology of the drugs in relation to their molecular structures and putative targets within the cAMP signaling system.

2. Materials and methods

2.1. Materials

Carbamazepine (CBZ; cat. no.: C4024), oxcarbazepine (OXC; O3764), eslicarbazepine acetate (ESL; B5435), 3-isobutyl-1-methylxanthine (IBMX; I5879), mouse anti-vinculin antibody (V9131), mouse anti-FLAG antibody (F1804), Ponceau-S solution (P7170) and penicillin-streptomycin (P4333) were purchased from Sigma Aldrich (St. Louis, MO, USA). Fetal bovine serum was purchased from Invitrogen A/S (Taastrup, Denmark). Zeocin selective antibiotic (ant-zn-1) was purchased from Invivogen (San Diego, CA, USA). Amersham ECL Prime Western Blotting Detection Reagent (RPN2232) was purchased from GE Healthcare Life Sciences (Chicago, IL, USA). Licarbazepine (LIC; racemic mixture; ab145867), 10X RIPA lysis buffer (ab156034) and rabbit anti-ADCY8 antibody (AB38336) were purchased from Abcam (Cambridge, United Kingdom). Mouse anti-CREB antibody (sc-377154) and mouse anti-p-CREB antibody (sc-81486) were purchased from Santa Cruz Biotechnology (Dallas, TX, USA). Polyclonal secondary horseradish peroxidase (HRP)-conjugated goat anti-mouse antibody (P0447) and swine anti-rabbit antibody (P0217) were obtained from Agilent, former Dako (Glostrup, Denmark). Thapsigargin (1138), forskolin (FSK; 1099) and isoprenaline (ISO; 1747) were purchased from Tocris (Bristol, United Kingdom). Nunc™ F96 MicroWell™ Black Polystyrene plate (137101), Lipofectamine™ 2000 Transfection Reagent (11668-019), Halt Protease/Phosphatase Inhibitor Cocktail 100x (78442), Micro BCA Protein Assay Kit (23235), 4x NuPAGE MOPS LDS sample buffer (NP 0007), NuPAGE running buffer (NP 0001), NuPAGE antioxidant (NP 0005), NuPAGE transfer buffer (NP 0006), MagicMark™ XP Western Protein Standard (LC 5602), NuPAGE® 4–12% Bis-Tris gel (NP 0322) Pierce™ ECL Western Blotting Substrate (32209) and SuperSignal™ West Femto Maximum Sensitivity Substrate (34095) were purchased from Thermo Fisher Scientific (Waltham, MA, USA). Precision Plus Protein™ Dual Color standards (1610374) was purchased from Bio-Rad (Hercules, CA, USA). All other chemicals were used of appropriate purity from commercial sources.

2.2. Cell culturing

HEK293 cells stably expressing the Förster resonance energy transfer (FRET)-based cAMP biosensor, Epac149 (hereafter simply designated HEK293 cells), a kind gift from Dr. Jesper M. Mathiesen (University of Copenhagen, Denmark, and Zealand Pharma, Glostrup, Denmark), were utilized for all experiments. HEK293 cells were maintained in DMEM supplemented with 10% fetal bovine serum, 1% penicillin-streptomycin and 2 mM L-glutamine at 37 °C with 5% CO_2/95% air, later referred to as culture medium. 60 μg/ml Zeocin was employed for selection and maintenance of the HEK293 cells, and the cultures were employed for experiments at approximately 80–90% confluency and between 2 and 23 passages from the batch obtained from Dr. Mathiesen.

2.3. Transient expression of AC8

HEK293 cells were transfected at ~80–90% confluency using a lipid-based transfection method. A FLAG-tagged rat AC8 pcDNA3.0 construct, a kind gift from Dr. Michelle Halls (Monash Institute of Pharmaceutical Sciences, Monash University, Melbourne, Australia), was transfected into HEK293 cells with a DNA (μg):Lipofectamine® 2000 Reagent (μl) ratio of 1:6. Transfection took place for 6 h before transfection medium was replaced with culture medium and the transfected cells were employed for experiments 36–48 h post-transfection. Successful transfection was verified by western blotting utilizing mouse anti-FLAG

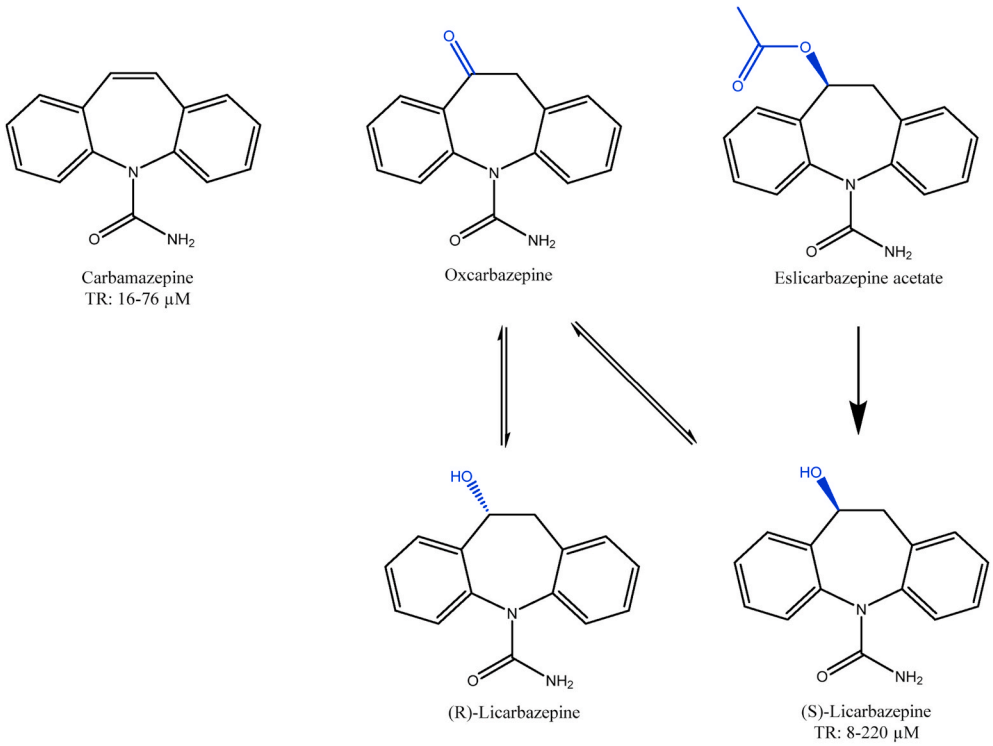

Fig. 1. Chemical structures of carbamazepine (CBZ) and its structural derivatives, oxcarbazepine (OXC) or eslicarbazepine acetate (ESL). OXC is reversibly converted into (R)-licarbazepine and (S)-licarbazepine while ESL is only converted into (S)-licarbazepine; however, a small amount undergoes chiral inversion to (R)-licarbazepine through oxidation to OXC. Therapeutic range (TR) is expressed as concentration in plasma for CBZ or (S)-licarbazepine only since no data were available for the other compounds due to extensive metabolism. Differences between the molecular structures are highlighted in blue. See text for details and references.

antibodies. FLAG-AC8 transfected cells will later be referred to as AC8-HEK293 cells.

2.4. Real-time plate-based cAMP assay

To investigate the effects of CBZ, OXC, ESL or LIC on accumulation of cAMP in HEK293 cells, three different protocols were applied. Following a 10-min preincubation with the drug under investigation, synthesis of cAMP was stimulated for 30 min with either ISO, FSK or, for AC8-HEK293 cells, by inducing store-operated Ca^{2+} entry (SOCE) as elaborated below. The accumulation of cAMP was monitored employing a fluorescence-based assay in a 96-well plate reader-format at 37 °C. Accumulation of cAMP was calculated as the area under the curve during the 30-min period and expressed as FRET ratio x min for statistical analysis.

2.5. FSK/ISO-mediated cAMP accumulation

Black 96-well plates with a clear, flat bottom were prepared with CBZ, OXC, ESL or LIC diluted in HBS buffer (1 mM $MgCl_2$, 4 mM KCl, 20 mM HEPES, 11 mM glucose, 140 mM NaCl, 1 mM $CaCl_2$, pH 7.4) to reach final concentrations of 1, 10 or 100 μM. FSK or ISO were also diluted in HBS buffer to reach final concentrations of 5 or 0.1 μM, respectively. HEK293 cells resuspended in HBS buffer were added to the plate and incubated with the drug under investigation for 10 min prior to addition of FSK or ISO to induce cAMP accumulation.

2.6. Ca^{2+}-mediated cAMP accumulation

Black 96-well plates with a clear, flat bottom were prepared with CBZ, OXC, ESL or LIC diluted in Ca^{2+}-free HBS buffer supplemented with 0.1 mM EGTA to reach final drug concentrations of 1, 10 or 100 μM. $CaCl_2$ were diluted in Ca^{2+}-free HBS buffer and thapsigargin were diluted in Ca^{2+}-free HBS buffer +0.1 mM EGTA to reach final concentrations 1.8 mM and 1 μM, respectively. Approximately 20 min before AC8-HEK293 cells were employed for experiments, the culture medium was replaced with Ca^{2+}-free HBS buffer +0.1 mM EGTA to remove extracellular unbound Ca^{2+}. AC8-HEK293 cells resuspended in Ca^{2+}-free HBS buffer +0.1 mM EGTA were added to the plate and incubated with the drug under investigation for 4 min prior to addition of thapsigargin for 6 min to deplete endoplasmic reticulum Ca^{2+} stores. After a total of 10 min of incubation with the drug under investigation, Ca^{2+} (final concentration; f.c. 1.8 mM) were added to the wells to induce SOCE and thus cAMP accumulation catalyzed by AC8.

2.7. FRET-based cAMP measurement

Immediately after addition of ISO/FSK/Ca^{2+}, the plates were placed in a SpectraMax *i*3x microplate reader (Molecular Devices, CA, USA) to measure real-time changes in cAMP dynamics expressed as changes in fluorescence intensity (settings: 37 °C; fluorescence readings every 2 min for 30 min; excitation for mCer was set at 430 nm; emission for mCer and mCit were read at 470 nm and 535 nm, respectively). Fluorescence intensity at 470 nm increases while fluorescence intensity at 535 nm decreases with increasing levels of cAMP. Thus, the FRET ratio decreases upon cAMP accumulation; however, to obtain traces which reflect the direction of change in cellular cAMP levels, the inverted FRET ratio was calculated by dividing fluorescence intensity at 470 nm with fluorescence intensity at 535 nm. To exclude data points caused by technical variation, FRET ratios below 0.85 and above 1.45 were excluded from the data analysis (based on baseline and maximum FRET ratios, respectively).

2.8. Validation of transient transfection of AC8 in HEK293 cells employing western blotting

36–48 h after transfection, the cells were briefly washed with PBS before being detached with 1 mM EDTA. Following centrifugation (200 g x 5 min), the pellet was resuspended in TNE lysis buffer (10 mM Tris, 150 mM NaCl, 1 mM EDTA, 5% Triton X-100, pH 8) with HALT protease/phosphatase inhibitor and the cells were lysed by repeatedly passing the cell suspension through a 23-gauge needle. The cell lysate was centrifuged at 20,000 g x 30 min x 4 °C, and the supernatant was transferred to a new tube and kept on ice for 30 min. The amount of protein was determined using a Micro BCA Protein Assay Kit according to the manufacturer's instructions. Samples were treated with NuPAGE MOPS LDS sample buffer and 50 mM dithiothreitol, vortexed and briefly spun down. Extracted proteins were separated on a NuPAGE® 4–12% Bis-Tris gel in a XCellSureLock™ mini-electrophoresis system (200 V, 80 min; Thermo Scientific, Waltham, MA, USA) in NuPAGE running buffer containing 1% antioxidant. The separated proteins were visualized using Ponceau-S staining prior to being transferred onto a 0.45 μm polyvinylidene difluoride (PVDF) membrane (30 V, 150 min) in NuPAGE transfer buffer containing 10% methanol and 0.1% NuPAGE antioxidant. To prevent non-specific binding of antibodies, the PVDF membrane was blocked at 4 °C overnight in 2% nonfat dried milk powder in a buffer containing 50 mM Tris, 100 mM NaCl, 2% Tween-20, pH 7.2. Subsequently, the membrane was incubated with monoclonal mouse anti-FLAG antibody (1:2000) at 4 °C overnight. The following day the membranes were incubated at room temperature for 90 min with polyclonal goat anti-mouse antibodies (1:2000) conjugated to horseradish peroxidase. The protein bands were visualized with Amersham ECL reagent according to the manufacture's instructions and detected on a Syngene Px*i* camera (Biocon, Bangalore, India).

2.9. Assessment of CREB phosphorylation by western blotting

HEK293 cells were treated with 100 μM CBZ for 10 min followed by incubation with FSK (f.c. 5 μM) for 30 min to assay for drug effects on phosphorylation of the endogenous transcription factor CREB. The treatments were terminated by removal of incubation buffer and HEK293 cells were lysed by addition of 100 μl ice cold 1x RIPA buffer. Cell lysates were boiled for 5 min at 95 °C, briefly sonicated and spun down at 12,500 g x 15 min x 4 °C. The amount of protein was determined using a Micro BCA Protein Assay Kit according to the manufacturer's instructions. Samples containing approximately 7.5 μg protein were treated with NuPAGE MOPS LDS sample buffer and 50 mM dithiothreitol and boiled at 95 °C for 10 min to denature and reduce proteins. The separation, transfer and blocking were performed as described above with slight alterations in running time (60 min) and transfer time (120 min). Subsequently, the membrane was cut at 75 kDa and the lower part was incubated with monoclonal mouse anti-CREB antibodies (1:500) or mouse anti-p-CREB antibodies (1:1000), while the upper part was incubated with monoclonal mouse anti-vinculin antibody (1:1000) at 4 °C overnight prior to being incubated at room temperature for 90 min with polyclonal goat anti-mouse (1:1000) antibodies conjugated to HRP. The protein bands were visualized with West femto (CREB and P-CREB) or Pierce ECL reagent (Vinculin) according to manufactures' instructions and detected on a Syngene Px*i* camera. Band intensity was quantified using ImageJ (RRID: SCR_003070). The quantified bands of interest were normalized to the respective vinculin band. The data are presented as the ratio between phosphorylated protein and total protein, and each n represents individual experiments performed on individual batches of cells. Linearity between loaded cell lysate (in the range 4–12 μg protein) and band intensity was verified for vinculin, CREB and phosphorylated CREB (data not shown). Furthermore, vinculin was compared to total protein staining by Ponceau-S which revealed that the treatment had no effect on the expression of vinculin (data not shown).

2.10. Data analysis

Statistical significance was assessed by repeated measures ANOVA with Dunnett's multiple comparisons post-test (for the FRET-based cAMP measurements) or by repeated measures ANOVA with Tukey's multiple comparisons post-test (for the CREB phosphorylation quantification). $P \leq 0.05$ is considered to be statistically significant. Details on the ANOVA including P-values and degrees of freedom for the cAMP accumulation experiments are given in supplementary Table T1. In all cAMP accumulation experiments performed, the degrees of freedom for the Dunnett's multiple comparisons post-test are 4 and for the statistical analysis of the western blots presented in Fig. 3, the degrees of freedom for the Tukey's multiple comparisons test are 3. For all data derived from the HEK293 cell line, n indicates the number of biological replicates defined as an independent experiment performed on a separate day with freshly made solutions, reagents and drugs in accordance with Lazic et al. (2018). Data were analysed and presented using Microsoft Excel (RRID:SCR_016137) and GraphPad Prism v.8 software (RRID: SCR_002798).

3. Results

To investigate the effects of the drugs under investigation on cAMP accumulation, a HEK293 cell line stably expressing a FRET-based cAMP biosensor was employed as model system (Vedel et al., 2015). Native HEK293 cells express the necessary components for studying cAMP accumulation and has previously been employed for this purpose (Uhlén et al., 2015; Vedel et al., 2015). Furthermore, the genotypic and phenotypic profiles of HEK293 cells are heterogenous and not consistent with their supposed nephrological origin; in fact, they express several proteins normally associated with neurons and may thus be considered a reasonable pseudo-CNS model system (Shaw et al., 2002; Supplementary Fig. S1). Following a 10-min preincubation with either one of the four compounds, accumulation of cAMP was induced by addition of forskolin (FSK; direct activator of AC catalytic activity; 5 μM) or isoprenaline (ISO; unselective β receptor agonist; 0.1 μM) and the accumulation of cAMP was monitored for 30 min and quantified as the area under the curve (FRET ratio x min; see the Materials and methods section and Fig. 2A,B). The effect on cAMP accumulation of the four compounds were all tested at three different concentrations, 1, 10, or 100 μM. We decided on these concentrations based on previous studies investigating the effects of CBZ on cAMP accumulation in similar *in vitro* systems (Chen et al., 1996; Ferrendelli and Kinscherf, 1979; Mann et al., 2009) and on the clinically relevant plasma levels of CBZ (17–76 μM; calculated from Arroyo and Sander, 1999). FSK was employed to produce a global cellular rise in cAMP by activating the ACs present whereas ISO was employed to produce G-protein-coupled receptor-linked cAMP accumulation (Ellisdon and Halls, 2016; Halls, 2018). We based the employed concentrations of FSK or ISO on previous work in similar cell-based systems (Mathiesen et al., 2013; Müller et al., 2014) and subsequently adjusted to concentrations which did not saturate the biosensor while still producing a potent cAMP signal. The representative response kinetics of the two different AC-activation protocols are shown in Fig. 2B and the traces represent basal levels of cAMP in HEK293 cells or cells treated with either 20 μM FSK +100 μM 3-isobutyl-1-methylxanthine (IBMX; reflects saturation of the biosensor,

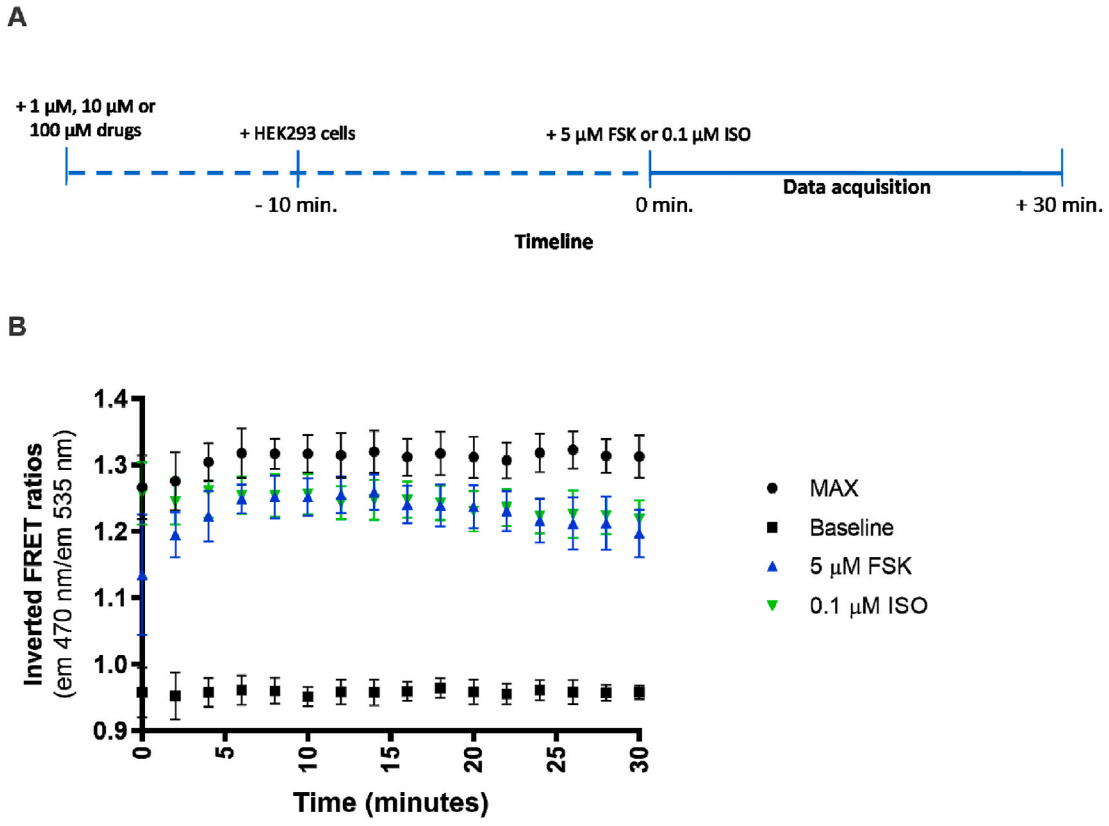

Fig. 2. Induction of cAMP accumulation in HEK293 cells. **A** The 96-well plates were prepared with the drugs under investigation prior to addition of cells. Reading of the plate was initiated upon addition of forskolin (FSK; activates adenylyl cyclases) or isoprenaline (ISO; β receptor agonist) following 10 min of preincubation and the plate was read for 30 min with 2 min intervals. **B** In principle, the FRET ratio decreases upon increasing cAMP levels. However, to display a trace that reflects the direction of changes in cAMP levels, the inverted FRET ratio was calculated and depicted instead (Mathiesen et al., 2013; Vedel et al., 2015). See the Materials and methods section for further details. Baseline cAMP levels are shown along with the maximal (MAX) cAMP response induced with a cocktail of 20 μM FSK plus 100 μM 3-isobutyl-1-methylxanthine (IBMX; blocks phosphodiesterases) reflecting saturation of the biosensor. cAMP responses mediated by 5 μM FSK or 0.1 μM ISO are shown in blue and green, respectively. The data are presented as means ± S.D. of a representative experiment with 12 technical replicates.

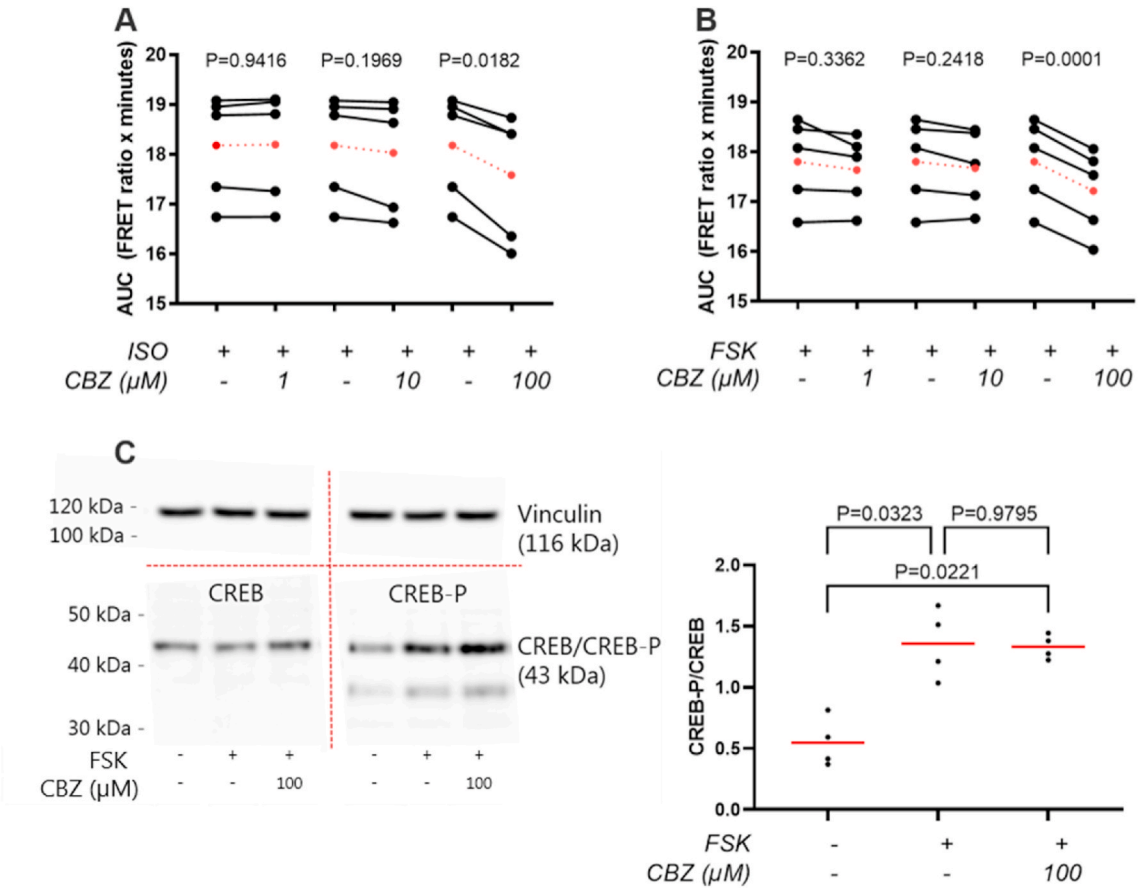

Fig. 3. Carbamazepine (CBZ) attenuates cAMP accumulation in HEK293 cells. The cells were pre-treated with 1 μM, 10 μM or 100 μM CBZ and then stimulated with either 0.1 μM isoprenaline (ISO; panel **A)** or 5 μM forskolin (FSK; panel **B**) for 30 min. See the text, the Materials and methods section and Fig. 2 for further experimental details. 100 μM CBZ significantly ($P \leq 0.05$) attenuated both ISO- and FSK-mediated cAMP accumulation. Data are presented as comparisons of non-treated and CBZ-treated cells ($n = 5$ with each data point representing the average of 6–12 technical replicates). Means are shown as red dotted lines and data were analysed employing repeated measures ANOVA with Dunnett's multiple comparisons post-test. **C** Under identical assay conditions, western blot analysis revealed that FSK treatment significantly increased phosphorylation of CREB ($P \leq 0.05$) while CBZ (100 μM) had no effect on this. Data are presented as the ratio between CREB-P and CREB after the band intensities were normalized to the respective vinculin bands (loading control; $n = 4$). Means are shown as red lines and data were analysed employing repeated measures ANOVA with Tukey's multiple comparisons post-test.

MAX), 0.1 μM ISO or 5 μM FSK, respectively. The two latter both produced a level of cAMP accumulation showing no saturation of the biosensor meaning that we would be able to detect both increases and decreases in cAMP accumulation as a consequence of the presence of the four drugs under investigation. All data presented below are analysed and presented according to good practices for analyzing and presenting pharmacological data and western blots (Fosang and Colbran, 2015; Lew, 2007; Weissgerber et al., 2017).

3.1. CBZ inhibits cAMP accumulation in HEK293 cells confirming the validity of the assay

It has previously been demonstrated that CBZ is able to attenuate cAMP accumulation (e.g. Chen et al., 1996; Mann et al., 2009). To test if we could reproduce these findings in our HEK293 model system, the cells were pretreated for 10 min with three different concentrations of CBZ (1, 10 or 100 μM) and then treated for 30 min with either 5 μM FSK or 0.1 μM ISO to induce cAMP accumulation (as explained above and in the Materials and methods section). 100 μM CBZ (FSK, $P = 0.0182$; ISO $P = 0.0001$), but not 1 (FSK, $P = 0.9416$; ISO, $P = 0.3362$) or 10 μM (FSK, $P = 0.1969$; ISO $P = 0.2418$), significantly attenuated both ISO- and FSK-mediated cAMP accumulation (Fig. 3A,B). Thus, we were able to confirm that CBZ attenuates cAMP accumulation showing that our assay is able to report changes in cAMP accumulation as shown with orthogonal methods in other studies. To test if downstream cAMP-mediated events are activated in the HEK293 cells by the level of cAMP accumulation induced, we investigated the ability of FSK to stimulate phosphorylation of the transcription factor cAMP response element-binding protein (CREB; Mertz et al., 2020). We employed a protocol similar to the one employed for the cAMP accumulation assay and probed the phosphorylation ratio of CREB by western blotting. We find that FSK significantly increases the phosphorylation ratio of CREB ($P = 0.0323$; Fig. 3C). However, the additional presence of CBZ (100 μM) does not attenuate the FSK-induced phosphorylation of CREB ($P = 0.9795$) under the conditions investigated suggesting that CBZ does not attenuate the cAMP signal sufficiently to affect downstream CREB signaling (Fig. 3C). Thus, the cAMP assay conditions employed here are able to reproduce earlier findings meaning that we may employ the assay to investigate the effects of the structural derivatives of CBZ on cAMP accumulation. However, any downstream effects on CREB phosphorylation may not be detected in this model system and was thus not further explored.

3.2. OXC, ESL and LIC show distinct effects on cAMP accumulation in HEK293 cells

Despite the fact that we have known about CBZ's effect on cAMP signals for decades, the potential of the newer structural derivatives, OXC or ESL, to affect cAMP accumulation have not been investigated. We therefore questioned, based on the similar structures, whether OXC,

ESL or their common metabolite, LIC, would exert similar effects as CBZ or if the hydrophilic substitution on the heterocyclic ring would disrupt a potential hydrophobic interaction with the ACs (see Fig. 1). Employing a similar experimental setup as above, we saw no significant effects of OXC on ISO- (1 μM, P = 0.5370; 10 μM, P = 0.3273; 100 μM, P = 0.2435) or FSK-mediated (1 μM, P = 0.4592; 10 μM, P = 0.4757; 100 μM, P = 0.0504) cAMP accumulation at any concentration (Fig. 4A). Surprisingly, and in contrast to CBZ, 100 μM ESL (P = 0.0075) significantly enhanced ISO-mediated cAMP accumulation while 1 (P = 0.9128) and 10 μM (P = 0.4047) had no effect (Fig. 4B). ESL also significantly enhanced FSK-mediated cAMP accumulation; however, in a reversed or U-shaped concentration-response relationship with 1 (P = 0.0092) and 10 μM (P = 0.0132) significantly enhancing cAMP accumulation whereas 100 μM (P = 0.8047) exhibited no significant effects (Fig. 4B). Finally, the active metabolite LIC displayed no significant effects on neither ISO- (1 μM, P = 0.7101; 10 μM, P = 0.9848; 100 μM, P = 0.8314) nor FSK-mediated (1 μM, P = 0.4879; 10 μM, P = 0.5786; 100 μM, P = 0.8178) cAMP accumulation (Fig. 4C) despite the structural resemblance to both CBZ, OXC and ESL. Thus, the structural derivatives of CBZ show diverse effects on cAMP accumulation in HEK293 cells with ESL

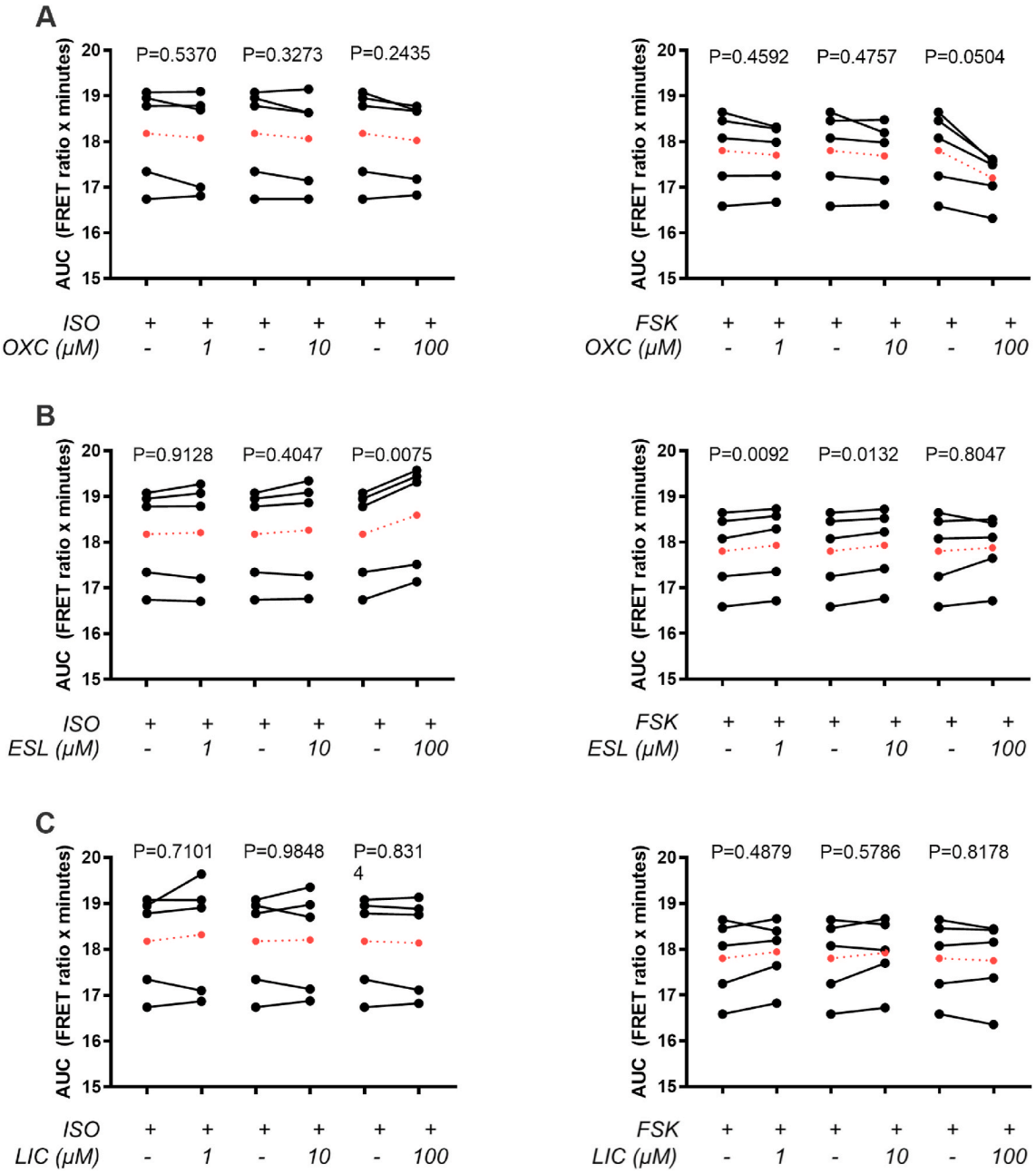

Fig. 4. Oxcarbacepine (OXC), eslicarbazepine acetate (ESL) or licarbazepine (LIC) show distinct effects on cAMP accumulation in HEK293 cells. The cells were pre-treated with 1 μM, 10 μM or 100 μM OXC (**A**), ESL (**B**) or LIC (**C**), respectively, and then stimulated with either 0.1 μM isoprenaline (ISO) or 5 μM forskolin (FSK) for 30 min. See the text, the Materials and methods section and Fig. 2 for further experimental details. OXC showed no significant effects on ISO-mediated cAMP accumulation whereas 100 μM OXC exhibited a trend (P≤0.075) towards attenuating FSK-mediated cAMP accumulation. 100 μM ESL significantly (P≤0.05) increased ISO-mediated cAMP accumulation. When stimulating cAMP accumulation with FSK, 1 μM and 10 μM ESL significantly increased cAMP accumulation whereas 100 μM had no significant effect. The active metabolite LIC demonstrated no effects on neither ISO- nor FSK-mediated cAMP accumulation. Data are presented as comparisons of non-treated and drug-treated cells (n = 5 with each data point representing the average of 6–12 technical replicates). Means are shown as red dotted lines and data were analysed employing repeated measures ANOVA with Dunnett's multiple comparisons post-test.

showing not only a surprising increase in cAMP accumulation but also a complex dose-response relationship. It is important to note that OXC and ESL are metabolized rapidly to LIC (Almeida and Soares-da-Silva, 2007; Ambrósio et al., 2002; Bialer and White, 2010; May et al., 2003) leaving circulating amounts of OXC and ESL low at steady-state.

3.3. CBZ, OXC, ESL or LIC show distinct effects on cAMP accumulation in AC8-expressing HEK293 cells

In a previous study, we found that transcription of AC isoform 8 (AC8; *ADCY8*), as the only one of the nine plasmamembrane-bound AC isoforms, was upregulated in brain tissue from patients suffering from drug-resistant mesial temporal lobe epilepsy suggesting that this isoform could play a role in cAMP-driven epileptogenesis and/or propagation of seizures (Guelfi et al., 2019; Kjaer et al., 2019). Thus, we next decided to investigate if CBZ, OXC, ESL or LIC affects AC8-driven cAMP accumulation, specifically. We did not determine the exact endogenous expression of AC isoforms in the native HEK293 cell line; however, according to the literature, HEK293 cells express no endogenous AC8 (Uhlén et al., 2015; Supplementary Fig. S1). AC8, along with AC1 (low expression in HEK293 cells; Uhlén et al., 2015) are the only two isoforms of AC that are activated by Ca^{2+}/calmodulin (CaM) and responding selectively to Ca^{2+} entering *via* plasmamembrane channels such as that occurring during store-operated Ca^{2+} entry (SOCE), a process that operates to replenish the endoplasmic reticulum of Ca^{2+} *via* activation of Orai1 or/and TRP channels (Halls and Cooper, 2011). To investigate the effects of the four drugs on Ca^{2+}-driven, AC8-mediated cAMP accumulation, we transiently expressed a FLAG-tagged AC8 in the HEK293 cells using a conventional lipid-based transfection method (hereafter AC8-HEK293 cells). To activate AC8, we employed a protocol to induce SOCE that we have used previously in a different setting (Müller et al., 2014) briefly consisting of exposing the cells to thapsigargin (blocks reuptake of Ca^{2+} into the endoplasmic reticulum; 1 μM; 6 min) in the absence of extracellular Ca^{2+}; when Ca^{2+} (f.c. 1.8 mM) is re-introduced in the buffer solution, SOCE is activated (see the Materials and methods section for details and Fig. 5A). This protocol induced accumulation of cAMP in AC8-HEK293 cells but not in the parent HEK293 cells, suggesting no endogenous AC8 (or AC1) expression in the parent cells (Fig. 5B). We further confirmed AC8-expression by western blotting (Fig. 5C). FLAG-AC8 was visualized as several diffuse bands; the bands ~120 kDa were slightly lower than the expected molecular weight of 140 kDa of AC8. The bands at ~140 kDa are presumably a glycosylated form of AC8, while the bands above 220 kDa suggest a dimeric form of AC8 – both in the non-glycosylated and glycosylated form. Previous studies have shown that dimeric forms of AC8 can persist during gel electrophoresis (Pagano et al., 2009). Dimeric/oligomeric forms of AC8 might be a consequence of overexpression of AC8; yet, studies have shown that dimeric forms of AC8 are also observed in an endogenous setting (Gu et al., 2002; Pagano et al., 2009). Dimeric/oligomeric forms of AC8 should in principle not be detected since the protein samples were both reduced and denatured before loading onto the gel. However, to limit aggregation of the hydrophobic AC8 molecules, the protein samples were not boiled before loading onto the gel which could mean that complete reduction and denaturing were hampered. As expected, no FLAG signal was detected in the negative control. As before, the AC8-HEK293 cells were pretreated for 10 min with three different concentrations of either CBZ, OXC, ESL or LIC (1, 10 or 100 μM). Similar to what was observed in the parent HEK293 cells 1 ($P = 0.9999$) and 10 μM CBZ ($P = 0.9454$) showed no effect on cAMP accumulation while it was lowered by 100 μM ($P = 0.0166$; Fig. 6A). In contrast to what was observed in the parent HEK cells OXC 1 ($P = 0.0212$) and 10 μM ($P = 0.0423$) were able to attenuate cAMP accumulation mediated by AC8 while 100 μM ($P = 0.2375$) had no effect (Fig. 6B). ESL at 10 ($P = 0.0271$) and 100 μM ($P = 0.0164$) increased cAMP accumulation while 1 μM ($P = 0.1760$) had no effect (Fig. 6C). LIC showed no effect on AC8 mediated cAMP accumulation (1 μM, $P = 0.9739$; 10 μM, $P = 0.9999$; 100 μM, $P = 0.7024$). In general, the data show the same overall trend as in the parent HEK293 cells with one significant difference; OXC is able to attenuate cAMP accumulation mediated by AC8 at 1 and 10 μM but not at 100 μM (Fig. 6B). This finding is in contrast to activation by FSK/ISO in the parent HEK293 cells where only a near-significant attenuation is seen for the FSK-induced signal at 100 μM OXC (Fig. 4A). This shift in sensitivity between the parent HEK293 cells and AC8-HEK293 cells to the action of OXC suggests that OXC, like ESL, show a complex pharmacological profile with regards to AC8 possibly exhibiting a U-shaped dose-response relationship.

4. Discussion

The underlying molecular mechanism of epileptogenesis is poorly understood but is believed to be a process progressing over several years providing a wide window for antiepileptogenic intervention (Devinsky et al., 2018) and both short-term effects (phosphorylation of proteins implicated in immediate neuronal excitability) and long-term effects (altered gene expression profiles) of cAMP signaling have been suggested to be involved (review, Mertz et al., 2020).

4.1. No correlation between clinical efficacy and effects on cAMP accumulation

Increased cAMP levels are associated with enhanced epileptiform activity (Higashima et al., 2002; Zhang et al., 2017). Thus, the ability of CBZ or OXC to inhibit cAMP accumulation, for the latter the potential pathologically relevant AC8-mediated signals (Mertz et al., 2020), could theoretically bring about alterations in both immediate and long-term neuronal excitability (Vazquez-Lopez et al., 2005; Zhu et al., 2015, 2012). Yet, OXC and ESL display similar clinical efficacies in the treatment of epilepsy (Almeida and Soares-da-Silva, 2007; Ambrósio et al., 2002; May et al., 2003). One possible explanation for this is that at steady-state, OXC or ESL predominantly exist in the circulation as the common active metabolite, LIC, which showed no effects on cAMP accumulation. First-pass metabolism of OXC or ESL to LIC is extensive (Bialer and White, 2010) and the therapeutic range for LIC corresponds to total plasma concentrations (not considering the significant protein binding) ranging from 8 to 220 μM (Arroyo and Sander, 1999; Bring and Ensom, 2008). For CBZ, the attenuation of cAMP accumulation is only reached at 100 μM which is above the therapeutic range for CBZ, determined to be at total plasma concentrations ranging from 17 to 76 μM (Arroyo and Sander, 1999; Bring and Ensom, 2008).

In summary, three observations presented here suggest that there is no simple or direct correlation between the drugs' effect on cAMP signaling and their clinical efficacy in epilepsy: i) The three parent drugs, CBZ, OXC or ESL, have distinct effects in terms of the direction in which they manipulate cAMP accumulation; ii) LIC, the dominating active metabolite of OXC and ESL, have no effect on cAMP accumulation; iii) CBZ only works at concentrations outside the clinically relevant range.

This conclusion, however, does not discredit cAMP signaling *per se* as a putative disease-modifying drug target in epilepsy. Drugs with improved affinity for proteins of the cAMP signaling pathways and/or targeting specific cAMP signals such as that generated by AC8, might prove to be able to modify relevant downstream events (Mertz et al., 2020). Interestingly, D'antuono et al. (2010) found that in rat hippocampal slices where epileptiform activity was induced with the non-selective voltage-dependent potassium channel blocker 4-AP, 50 μM CBZ inhibited ictal-like events but had no effect on the interictal-like discharges. However, when the concentration was raised to 200 μM, a level where effects on cAMP signaling are likely to occur (cf. our data), the frequency of the interictal-like discharges was decreased (D'Antuono et al., 2010). Thus, it is tempting to speculate that this change in frequency could be due to the effects on cAMP signaling and not effects related to voltage-gated sodium channels.

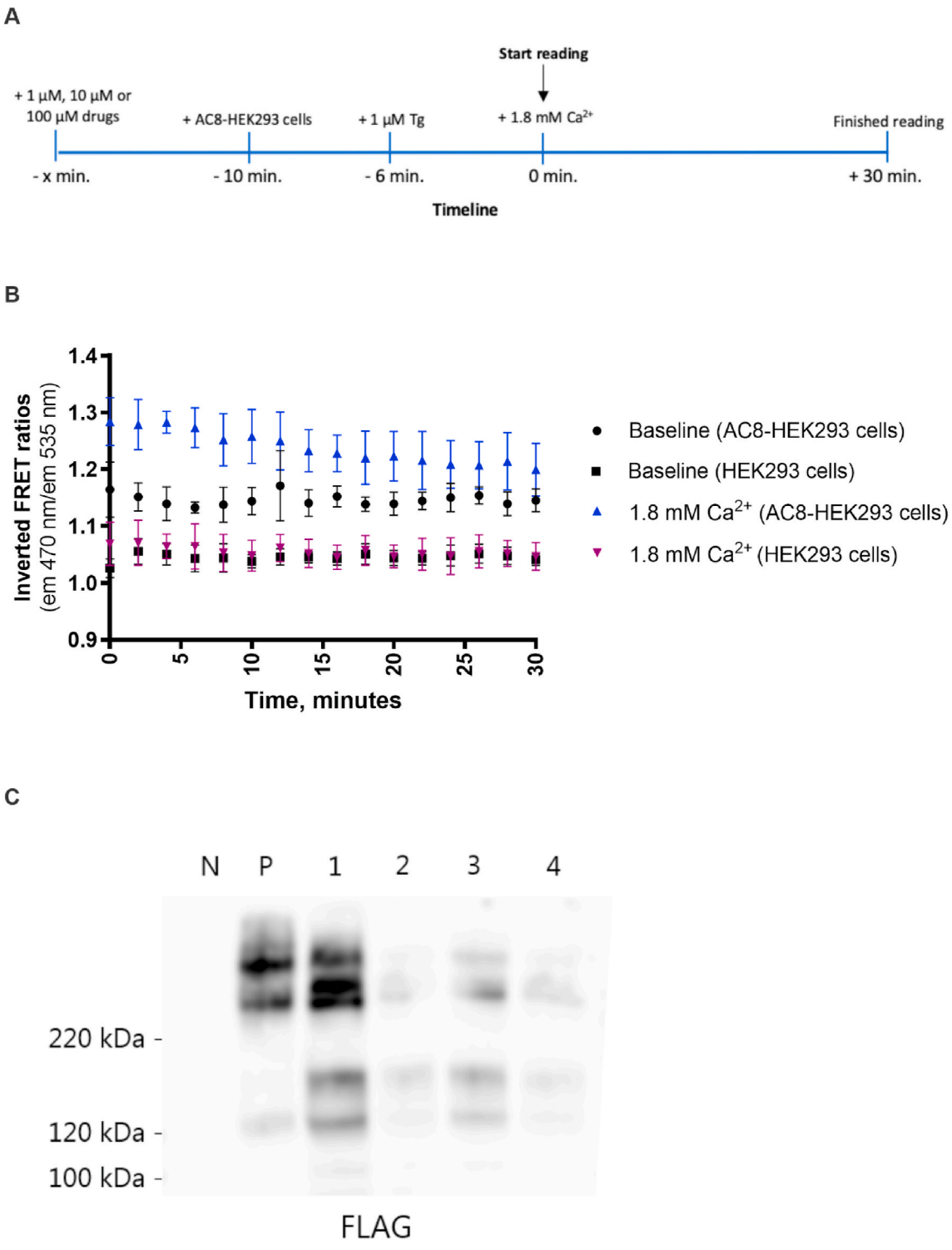

Fig. 5. Induction of Ca^{2+}-mediated cAMP accumulation in AC8-expressing HEK293 cells (AC8-HEK293). **A** Timeline showing the experimental protocol for testing the effects of the drugs under investigation on cAMP accumulation induced by store-operated Ca^{2+} entry (SOCE) in AC8-HEK293 cells. Both parent HEK293 cells and AC8-HEK293 cells were treated with 0.1 µM thapsigargin (Tg) for 6 min followed by addition of 1.8 mM Ca^{2+} to induce SOCE. **B** A transient rise in cAMP levels followed SOCE in AC8-HEK293 cells (blue) in accordance with AC8 being stimulated by Ca^{2+} influx. A similar rise was not observed in parent HEK293 cells (purple). The data are presented as means ± S.D. and are representative of three individual experiments with 6 technical replicates. **C** To validate the expression of AC8, western blotting of cell lysates of the AC8-HEK293 cells used for these experiments were performed employing an antibody against the FLAG-tag on the expressed AC8 (see the Materials and methods section for details). From the left: N = negative control (non-transfected HEK293 cells), P = positive control (AC8-transfected HEK293 cells), 1–4 = the four individual experiments in Fig. 6.

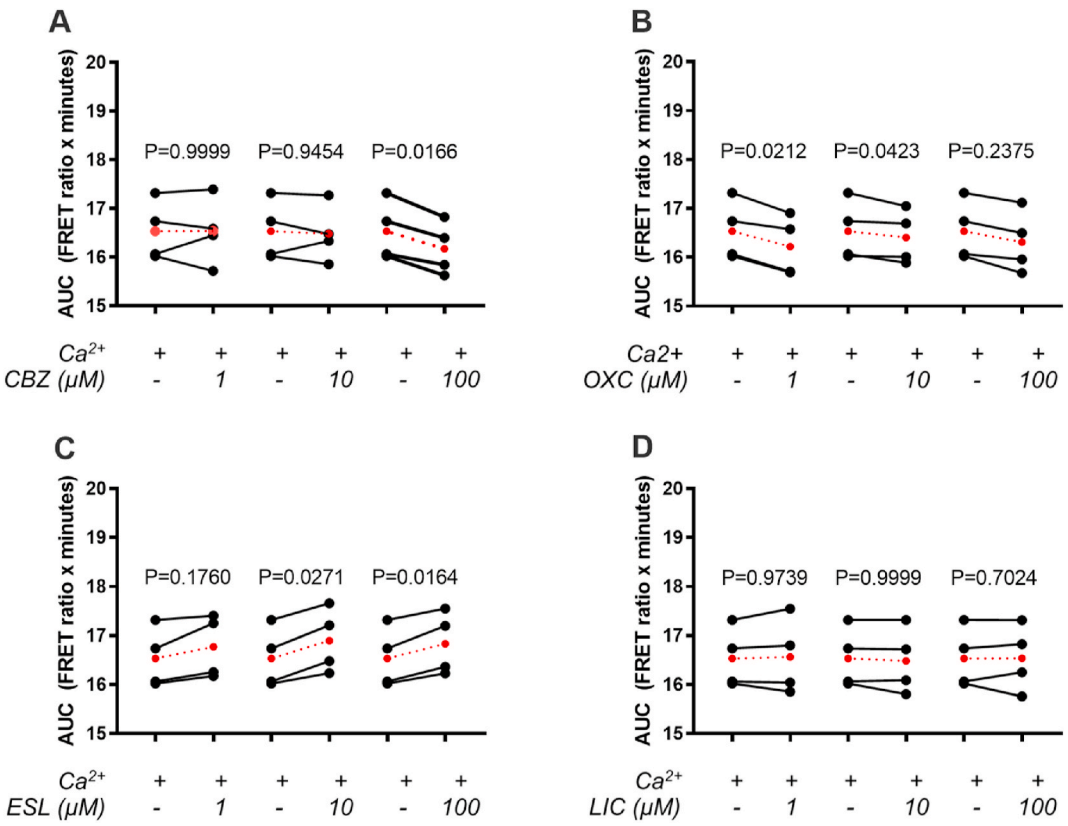

Fig. 6. Effect of carbamazepine (CBZ), oxcarbazepine (OXC), eslicarbazepine (ESL) or licarbazepine (LIC) on AC8-mediated cAMP accumulation induced by store-operated Ca^{2+} entry (SOCE; indicated as Ca^{2+}). AC8-HEK293 cells were pre-treated with 1 μM, 10 μM or 100 μM CBZ (**A**), OXC (**B**), ESL (**C**) or LIC (**D**), respectively, prior to inducing cAMP accumulation by SOCE (as detailed in Fig. 5 and the Materials and methods section). 100 μM CBZ significantly ($P \leq 0.05$) attenuated cAMP production as did 1 μM and 10 μM but not 100 μM of OXC. 10 μM and 100 μM ESL increased cAMP accumulation ($P \leq 0.05$) and LIC demonstrated no effects. Data are presented as comparisons of non-treated and drug-treated cells (n = 4 with each data point representing the average of 6–12 technical replicates). Means are shown as red dotted lines and data were analysed employing repeated measures ANOVA with Dunnett's multiple comparisons post-test.

Finally, both CBZ and OXC have been shown effective in the treatment of affective disorders (Spina and Perugi, 2004) raising the possibility that the attenuation of cAMP accumulation could contribute to the therapeutic effects in the treatment of these conditions. Another possibility, of course, is that the effects on cAMP signaling contribute to the adverse rather than the therapeutic effects.

4.2. The effects of CBZ or OXC are probably mediated via direct interaction with ACs whereas ESL might act through interaction with PDEs

Despite the non-existent correlation to the clinical efficacy in epilepsy, it is of interest to learn the exact molecular mechanism by which the drugs under investigation here exert their effects on cAMP accumulation since this could be important for developing cAMP-directed therapeutics. We did not address this experimentally but several studies have investigated the mechanism-of-action for the inhibitory effect of CBZ on cAMP accumulation which might serve as a template for explaining the effects of OXC and ESL.

For CBZ, the effect appears to be at the level of cAMP production, not degradation, since attenuation of cAMP accumulation have been demonstrated in the presence of the non-selective phosphodiesterase (PDE)-inhibitor IBMX (Chen et al., 1996; Mann et al., 2009). AC activity is regulated in multiple ways with regulation by G protein-coupled receptors (GPCRs) being the best known. Thus, either inhibition of $G\alpha_s$- or activation of $G\alpha_i$-coupled receptors could be one mechanism-of-action by which CBZ attenuates cAMP accumulation. Indeed, CBZ has been suggested to interact with the G protein-coupled adenosine receptors (Ambrósio et al., 2002; Fujiwara et al., 1986). From our study, an effect on adenosine receptors cannot be ruled out since HEK293 cells express mRNA for adenosine receptors (Uhlén et al., 2015). However, a study by Chen et al. showed that uncoupling of the $G\alpha_i$-proteins from the receptors and thus inactivation of $G\alpha_i$-mediated signaling, had no effect on the inhibitory properties of CBZ on cAMP accumulation in C6 glioma cells (Chen et al., 1996). This suggests that the inhibitory effect of CBZ is independent of adenosine receptors or any other $G\alpha_i$-coupled receptor. Furthermore, to attenuate cAMP production *via* inhibition of $G\alpha_s$-coupled adenosine receptors, CBZ must be an antagonist/partial agonist. Since an antagonist/partial agonist needs the presence of an agonist, and there is no such in our experimental setup, inhibition of $G\alpha_s$-coupled adenosine receptors seem unlikely. Another possible mechanism-of-action by which CBZ inhibits cAMP accumulation is through direct action on ACs. Indeed, the study by Chen et al. reported that CBZ inhibits activity of purified ACs from rat cerebral cortex suggesting a direct interaction with AC (Chen et al., 1996). Further, CBZ does not seem to compete for the FSK binding site within the C1/C2 interface of the ACs (Chen et al., 1996); rather, a study by Mann et al. suggests that CBZ interacts with a hydrophobic catechol-estrogen binding pocket in the ACs thereby attenuating cAMP production (Mann et al., 2009). This hydrophobic patch is conserved among all mammalian transmembrane AC isoforms with both conserved and variable residues (Steegborn et al., 2005), and since CBZ is primarily hydrophobic in nature, a hydrophobic interaction seems highly possible.

Due to structural similarities, OXC, ESL and LIC could interact with the same hydrophobic binding pocket as CBZ. Yet, despite the structural similarities, they appear to exert complex and even opposing effects on cAMP accumulation. Since they only vary in a hydrophilic side group on the heterocyclic ring one would expect this substitution to be the reason for the observed distinct effects – unless, of course, they have distinct

targets. Due to the direct opposite effect of ESL compared to CBZ and OXC, it seems possible that ESL either stabilizes an active conformation of AC or affect a different target such as PDEs; ESL could inhibit PDE activity and thereby increase cAMP accumulation. There is no PDE inhibitor present in our experimental setup why an inhibitory effect on PDEs cannot be excluded.

Thus, the inhibitory properties of CBZ and OXC on cAMP accumulation is likely mediated *via* direct interaction with ACs whereas the ability of ESL to increase cAMP accumulation could be mediated *via* inhibition of PDEs.

4.3. The distinct effects can be explained by dissimilar polarity of the variable side-chain

Assuming that CBZ binds to the suggested hydrophobic catechol-estrogen binding pocket on the ACs, addition of a hydrophilic group to CBZ could potentially disturb a hydrophobic interaction and hence change the affinity/potency of the drugs. The structures of CBZ and OXC differs in a small hydrophilic side group, namely a ketone, on the heterocyclic ring (Fig. 1). That OXC only displays a trend towards decreasing FSK-mediated cAMP accumulation and had no effect on ISO-mediated cAMP accumulation could be an indication of the ketone moiety slightly, but not completely, disturbing a hydrophobic interaction between OXC and the endogenously expressed ACs in HEK293 cells. Surprisingly, it seems that the presence of the ketone leads to increased affinity for AC8 since the potency of OXC was higher than that of CBZ in AC8-HEK293 cells. ESL differs from CBZ in a methyl ester moiety located at the same place as the ketone on OXC. An ester moiety is less polar than a ketone (and a hydroxyl group) favoring a hydrophobic interaction compared to a ketone moiety. However, an ester moiety is also somewhat larger compared to a ketone. Thus, the ester moiety could create steric hindrance and thereby make the ESL-AC interaction less favorable than the OXC-AC interaction. It seems peculiar that two structurally similar molecules, only differing in a hydrophilic side group, would bind to the same place and induce opposing responses in an activated cAMP generating system. Regardless, CBZ and ESL exerted opposing effects. The study by Mann et al. suggests that CBZ has the potential to bind in several orientations within the hydrophobic catechol-estrogen binding pocket (Mann et al., 2009). Thus, in contrast to the above suggestion that ESL inhibits PDEs, the possibility does exist that the ester moiety favors a different orientation of ESL within the binding pocket letting the ester moiety interact with amino acid residues stabilizing a more active conformation of the ACs.

LIC has a hydroxyl group located at the same site as the ketone/ester on OXC/ESL, respectively. Compared to a ketone or an ester, a hydroxyl moiety is the more polar. Furthermore, the size of a hydroxyl moiety is somewhere between an ester and a ketone moiety. LIC demonstrated no effects on cAMP accumulation which could be explained by the size and the polar hydroxyl moiety making a hydrophobic interaction unfavorable and thus interrupting the hydrophobic interaction with the target.

In conclusion, the presence of the ketone in OXC seems to favor an inhibitory interaction selectively with AC8 over the endogenously expressed ACs. On the other hand, the ester moiety in ESL might provide it with the ability to stabilize an active conformation of AC, whereas the polarity of the hydroxyl group on LIC prevents it from binding to the ACs.

5. Conclusion

Our major novel finding is that there is no correlation between the clinical efficacy in epilepsy of CBZ, OXC or ESL and their ability to affect cAMP signaling *in vitro*. Thus, the effects on cAMP signaling is not likely to contribute to the therapeutic effects as it pertains to epilepsy. As discussed, the distinct effects on cAMP signaling of CBZ, OXC, ESL, or LIC are likely to be explained by differences in binding to the catechol-estrogen binding pocket on the ACs or, in the case of ESL, possible inhibition of PDEs. Clearly, more investigations are needed to elucidate the molecular pharmacology as this is could be important for further drug discovery efforts.

Our findings, however, do not discredit the notion of cAMP signaling *per se* as a viable drug target to treat epilepsy, as discussed here and as we have argued in detail in Mertz et al. (2020). Thus, we encourage the field to revisit cAMP as a drug target exploiting the knowledge about AC-based signaling hubs generated over the last decade or so (e.g. Calejo and Tasken, 2015; Cooper and Tabbasum, 2014; Dessauer, 2009; Ellisdon and Halls, 2016; Mertz et al., 2020; Reuschlein et al., 2019).

Author contributions and acknowledgements

SK, CM, EJ and SEHL performed experiments, data analysis and designed the experimental strategy in collaboration with LKB. LKB was the principal investigator and contributed, together with LHP, to the interpretation and discussion of the results. SK and CM wrote the draft manuscript and all authors contributed to the final version of the manuscript and proof-reading. The authors would like to acknowledge the technical assistance by Ms. Janet da Silva. The AC8 construct was a kind gift from Dr. Michelle Halls from the Monash Institute of Pharmaceutical Sciences, Monash University, Melbourne, Australia, who curates the construct library of professor Dermot Cooper, University of Cambridge, UK. The Epac149-expressing HEK293 cell line was a kind gift from Dr. Jesper M. Mathiesen, University of Copenhagen, Denmark, and Zealand Pharma (Glostrup, Denmark), based on the work published in Vedel et al. (2015). Financial support to SK from the Lundbeck Foundation *via* the Drug Research Academy at University of Copenhagen is cordially acknowledged. We are furthermore grateful for financial support from the Hørslev Foundation to LKB/CM, the Oda and Hans Svenningsen's Foundation for supporting LKB, and the Lundbeck Foundation for supporting EJ.

Declaration of competing interest

The authors declare no conflict of interest.

Appendix A. Supplementary data

Supplementary data to this article can be found online at https://doi.org/10.1016/j.ejphar.2020.173413.

References

Almeida, L., Soares-da-Silva, P., 2007. Eslicarbazepine acetate (BIA 2-093). Neurotherapeutics 4, 88–96.
Ambrósio, A.F., Soares-da-Silva, P., Carvalho, C.M., Carvalho, A.P., 2002. Mechanisms of action of carbamazepine and its derivatives, oxcarbazepine, BIA 2-093, and BIA 2-024. Neurochem. Res. 27, 121–130.
Arroyo, S., Sander, J.W., 1999. Carbamazepine in comparative trials: pharmacokinetic characteristics too often forgotten. Neurology 53, 1170–1174.
Bialer, M., White, H.S., 2010. Key factors in the discovery and development of new antiepileptic drugs. Nat. Rev. Drug Discov. 9, 68.
Bring, P., Ensom, M.H.H., 2008. Does oxcarbazepine warrant therapeutic drug monitoring? Clin. Pharmacokinet. 47, 767–778.
Calejo, A.I., Tasken, K., 2015. Targeting protein-protein interactions in complexes organized by A kinase anchoring proteins. Front. Pharmacol. 6, 192.
Chen, G., Pan, B., Hawver, D.B., Wright, C.B., Potter, W.Z., Manji, H.K., 1996. Attenuation of cyclic AMP production by carbamazepine. J. Neurochem. 67, 2079–2086.
Cooper, D.M., Tabbasum, V.G., 2014. Adenylate cyclase-centred microdomains. Biochem. J. 462, 199–213.
D'Antuono, M., Kohling, R., Ricalzone, S., Gotman, J., Biagini, G., Avoli, M., 2010. Antiepileptic drugs abolish ictal but not interictal epileptiform discharges in vitro. Epilepsia 51, 423–431.
Dessauer, C.W., 2009. Adenylyl cyclase–A-kinase anchoring protein complexes: the next dimension in cAMP signaling. Mol. Pharmacol. 76, 935–941.
Devinsky, O., Vezzani, A., O'Brien, T.J., Jette, N., Scheffer, I.E., de Curtis, M., Perucca, P., 2018. Epilepsy. Nature Reviews Disease Primers 4, 18024.
Ellisdon, A.M., Halls, M.L., 2016. Compartmentalization of GPCR signalling controls unique cellular responses. Biochem. Soc. Trans. 44, 562–567.

Ferrendelli, J.A., Kinscherf, D.A., 1979. Inhibitory effects of anticonvulsant drugs on cyclic nucleotide accumulation in brain. Ann. Neurol. 5, 533–538.
Fosang, A.J., Colbran, R.J., 2015. Transparency is the key to quality. J. Biol. Chem. 290, 29692–29694.
Fujiwara, Y., Sato, M., Otsuki, S., 1986. Interaction of carbamazepine and other drugs with adenosine (A1 and A2) receptors. Psychopharmacology 90, 332–335.
Gu, C., Cali, J.J., Cooper, D.M., 2002. Dimerization of mammalian adenylate cyclases. Eur. J. Biochem. /FEBS 269, 413–421.
Guelfi, S., Botia, J.A., Thom, M., Ramasamy, A., Perona, M., Stanyer, L., Martinian, L., Trabzuni, D., Smith, C., Walker, R., Ryten, M., Reimers, M., Weale, M.E., Hardy, J., Matarin, M., 2019. Transcriptomic and genetic analyses reveal potential causal drivers for intractable partial epilepsy. Brain 142, 1616–1630.
Halls, M.L., 2018. Localised GPCR signalling as revealed by FRET biosensors. Curr. Opin. Cell Biol. 57, 48–56.
Halls, M.L., Cooper, D.M.F., 2011. Regulation by Ca2+-signaling pathways of adenylyl cyclases. Csh Perspect Biol 3, 273–294.
Higashima, M., Ohno, K., Koshino, Y., 2002. Cyclic AMP-mediated modulation of epileptiform afterdischarge generation in rat hippocampal slices. Brain Res. 949, 157–161.
Kjaer, C., Barzaghi, G., Bak, L.K., Goetze, J.P., Yde, C.W., Woldbye, D., Pinborg, L.H., Jensen, L.J., 2019. Transcriptome analysis in patients with temporal lobe epilepsy. Brain 142, e55.
Lazic, S.E., Clarke-Williams, C.J., Munafo, M.R., 2018. What exactly is 'N' in cell culture and animal experiments? PLoS Biol. 16, e2005282.
Lew, M., 2007. Good statistical practice in pharmacology. Problem 2. Br. J. Pharmacol. 152, 299–303.
Mann, L., Heldman, E., Bersudsky, Y., Vatner, S.F., Ishikawa, Y., Almog, O., Belmaker, R. H., Agam, G., 2009. Inhibition of specific adenylyl cyclase isoforms by lithium and carbamazepine, but not valproate, may be related to their antidepressant effect. Bipolar Disord. 11, 885–896.
Mathiesen, J.M., Vedel, L., Bräuner-Osborne, H., 2013. Chapter eleven - cAMP biosensors applied in molecular pharmacological studies of G protein-coupled receptors. In: Conn, P.M. (Ed.), Methods in Enzymology. Academic Press, pp. 191–207.
May, T.W., Korn-Merker, E., Rambeck, B., 2003. Clinical pharmacokinetics of oxcarbazepine. Clin. Pharmacokinet. 42, 1023–1042.
Mertz, C., Krarup, S., Jensen, C.D., Lindholm, S.E.H., Kjaer, C., Pinborg, L.H., Bak, L.K., 2020. Aspects of cAMP signaling in epileptogenesis and seizures and its potential as drug target. Neurochem. Res. 45, 1247–1255.
Müller, M.S., Fox, R., Schousboe, A., Waagepetersen, H.S., Bak, L.K., 2014. Astrocyte glycogenolysis is triggered by store-operated calcium entry and provides metabolic energy for cellular calcium homeostasis. Glia 62, 526–534.
Pagano, M., Clynes, M.A., Masada, N., Ciruela, A., Ayling, L.-J., Wachten, S., Cooper, D. M.F., 2009. Insights into the residence in lipid rafts of adenylyl cyclase AC8 and its regulation by capacitative calcium entry. Am. J. Physiol. Cell Physiol. 296, C607–C619.
Palmer, G.C., Jones, D.J., Medina, M.A., Stavinoha, W.B., 1979. Anticonvulsant drug actions on in vitro and in vivo levels of cyclic AMP in the mouse brain. Epilepsia 20, 95–104.
Reuschlein, A.K., Jakobsen, E., Mertz, C., Bak, L.K., 2019. Aspects of astrocytic cAMP signaling with an emphasis on the putative power of compartmentalized signals in health and disease. Glia 67, 1625–1636.
Shaw, G., Morse, S., Ararat, M., Graham, F.L., 2002. Preferential transformation of human neuronal cells by human adenoviruses and the origin of HEK 293 cells. Faseb. J. 16, 869.
Spina, E., Perugi, G., 2004. Antiepileptic drugs: indications other than epilepsy. Epileptic Disord. 6, 57–75.
Steegborn, C., Litvin, T.N., Hess, K.C., Capper, A.B., Taussig, R., Buck, J., Levin, L.R., Wu, H., 2005. A novel mechanism for adenylyl cyclase inhibition from the crystal structure of its complex with catechol estrogen. J. Biol. Chem. 280, 31754–31759.
Uhlén, M., Fagerberg, L., Hallstrom, B.M., Lindskog, C., Oksvold, P., Mardinoglu, A., Sivertsson, A., Kampf, C., Sjostedt, E., Asplund, A., Olsson, I., Edlund, K., Lundberg, E., Navani, S., Szigyarto, C.A., Odeberg, J., Djureinovic, D., Takanen, J.O., Hober, S., Alm, T., Edqvist, P.H., Berling, H., Tegel, H., Mulder, J., Rockberg, J., Nilsson, P., Schwenk, J.M., Hamsten, M., von Feilitzen, K., Forsberg, M., Persson, L., Johansson, F., Zwahlen, M., von Heijne, G., Nielsen, J., Ponten, F., 2015. Proteomics. Tissue-based map of the human proteome. Science 347, 1260419.
Vazquez-Lopez, A., Sierra-Paredes, G., Sierra-Marcuno, G., 2005. Role of cAMP-dependent protein kinase on acute picrotoxin-induced seizures. Neurochem. Res. 30, 613–618.
Vedel, L., Bräuner-Osborne, H., Mathiesen, J.M., 2015. A cAMP biosensor-based high-throughput screening assay for identification of gs-coupled GPCR ligands and phosphodiesterase inhibitors. J. Biomol. Screen 20, 849–857.
Weissgerber, T.L., Savic, M., Winham, S.J., Stanisavljevic, D., Garovic, V.D., Milic, N.M., 2017. Data visualization, bar naked: a free tool for creating interactive graphics. J. Biol. Chem. 292, 20592–20598.
Zhang, Y., Gao, B., Zheng, F., Lu, S., Li, Y., Xiong, Y., Yang, Q., Yang, Y., Fu, P., Xiao, F., Wang, X., 2017. The phosphodiesterase 10A inhibitor PF-2545920 enhances hippocampal excitability and seizure activity involving the upregulation of GluA1 and NR2A in post-synaptic densities. Front. Mol. Neurosci. 10, 100-100.
Zhu, X., Dubey, D., Bermudez, C., Porter, B.E., 2015. Suppressing cAMP response element-binding protein transcription shortens the duration of status epilepticus and decreases the number of spontaneous seizures in the pilocarpine model of epilepsy. Epilepsia 56, 1870–1878.
Zhu, X., Han, X., Blendy, J.A., Porter, B.E., 2012. Decreased CREB levels suppress epilepsy. Neurobiol. Dis. 45, 253–263.